AIAA 2002-1369

Computation of Wrinkle Amplitudes in Thin Membranes

Y.W. Wong and S. Pellegrino
Department of Engineering, University of Cambridge, Cambridge CB2 1PZ, UK

43rd AIAA/ASME/ASCE/AHS/ASC Structures, Structural Dynamics, and Materials Conference
22-25 April 2002
Denver, CO

Computation of Wrinkle Amplitudes in Thin Membranes

Y.W. Wong* and S. Pellegrino†
Department of Engineering, University of Cambridge, Cambridge CB2 1PZ, UK

There is an increasing number of space missions in which it is proposed to use high accuracy membrane structures and it is envisaged that some of these membranes will remain partially wrinkled in their operational configuration. Previous studies have focussed only on the stress distribution in wrinkled membranes, but for high accuracy applications the amplitude and wavelength of the wrinkles becomes important. This paper presents a non-linear finite-element simulation technique, where the membrane is modelled in ABAQUS with S4R5 shell elements, which accurately predicts the wrinkle details. For a rectangular membrane in shear it is found that the wrinkled pattern varies abruptly when the load magnitude is changed gradually. This simulation technique makes it possible to "look inside" a membrane and thus identify features of the complex behaviour of thin membranes that need to be included in simple models, which can be very useful.

Introduction

There is an increasing number of space missions in which it is proposed to use high accuracy membrane structures with a variety of shapes and sizes. Examples are sunshields for low-temperature telescopes, space based radars, inflatable reflector antennas and solar sails.

Some of these membrane structures will remain partially wrinkled in their operational configuration, and this could potentially cause problems. For example, large wrinkles would compromise the performance of a sunshield or reflector, and could make a solar sail uncontrollable. However, wrinkles of smaller magnitude may be acceptable and, indeed, may even have beneficial effects, such as increasing the out-of-plane stiffness or the vibration damping of the membrane.

This paper presents a computational study of a wrinkled membrane in shear, a problem for which several solutions and experimental results have already been published. Initially the aim of this study was to explore the accuracy and robustness of a numerical simulation in which the membrane is modelled with a fine mesh of shell elements. It was later discovered that —due to the finite length of the membrane— the number of wrinkles varies abruptly with the shear displacement and this behaviour has the effect of introducing a certain amount of hysteresis in the system. The same numerical tools were then used to study the mode-jumping instability associated with this behaviour. Apart from being an interesting example of complex post-buckling response, it is possible that in future this behaviour could be exploited, e.g. for designing membrane structures with high vibration damping.

The paper begins with a brief review of previous studies of wrinkled membranes, which so far have focussed mainly on identifying the wrinkled regions and determining the magnitude of the tensile principal stresses. An analytical study by the current authors —leading to approximate expressions for the wrinkle wavelength and amplitude of infinitely long, uniformly sheared membranes— and an experimental study of square membranes subject to tension and shear, are particularly relevant to the present study.

Next, a non-linear finite-element simulation technique is presented, where the membrane is modelled in ABAQUS with S4R5 shell elements. The simulation consists of three main parts, namely (i) setting up an initial, lightly prestressed membrane; (ii) carrying out an eigenvalue analysis leading to the imperfection modes that are seeded into the membrane; and (iii) a post-wrinkling analysis with hand-tuned numerical stabilisation to go past the instabilities associated with mode jumping.

The following section presents a detailed numerical study of a particular rectangular membrane. Its overall behaviour is bilinear, depending on whether the membrane is flat or wrinkled, and is determined purely by the *tensile* principal stresses in the membrane. However, a more in-depth study of the ABAQUS results shows a complex variation in the shape of the membrane and the associated *compressive* stresses. Also, cycling the shear displacement back and forth produces an envelope of response curves —not a single one— thus indicating that any particular solution is unlikely to be unique.

Two separate validation studies are then presented, for a rectangular membrane in shear and a square membrane in tension and shear.

A discussion concludes the paper.

*Research Student.
†Professor of Structural Engineering, Associate Fellow AIAA. pellegrino@eng.cam.ac.uk

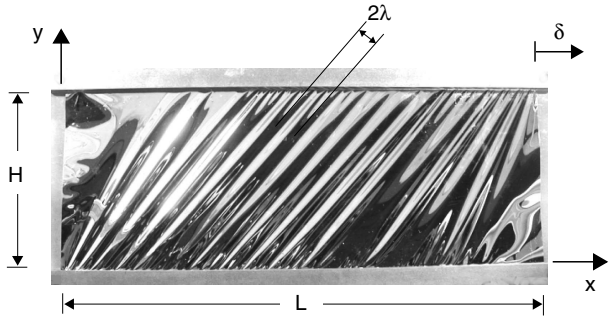

Fig. 1 Sheared Kapton foil with extensive wrinkling.

Background

Consider a thin, rectangular membrane of length L and height H. Let the horizontal edges be attached to rigid blocks held at a fixed distance and the vertical edges be free, and impose a purely horizontal translation of one of the two blocks. After only a very small displacement, wrinkles start to form in the membrane and, as the displacement is increased, the number of wrinkles increases and the out-of-plane deformation also increases.

Figure 1 shows a photograph of such a membrane. In the central part the wrinkles form a regular pattern, and the wavelength of the wrinkles, i.e. the separation between two consecutive troughs or crests, will be denoted by 2λ, see Figure 1.

Much work has already been done on the wrinkling of membranes; this work can be broadly divided into three different categories, which will be briefly reviewed next.

Analytical Approach

Most analytical studies so far have assumed that membranes have negligible bending stiffness and hence are unable to carry any compressive stresses.

The classical approach is the tension field theory, first introduced in 1929[1] for the analysis of thin webs in I-beams that are allowed to go much beyond their initial buckling load. In its original form, this theory considered a set of parallel wrinkle lines but later a simpler geometrical formulation was proposed,[2] which allowed for non-parallel tension rays. A further generalization[3,4] of this theory showed that the direction of the tension rays maximizes the (stretching) strain energy in the membrane. Closed form solutions for membranes with different shapes and anisotropic membranes were developed.

An alternative approach has been proposed for partly wrinkled membranes,[5] such as a pressurized cylindrical tube in pure bending. In this case the membrane can be divided into taut regions and wrinkled regions, and in the wrinkled region a variable Poisson's ratio can be defined such that there are no compressive stresses anywhere. Computer implementations of this approach will be mentioned in the next section.

A further approach considers finite elastic deformations of membranes with a special kind of strain energy density function, known as a relaxed strain energy. This function is zero if at least one principal stress is compressive.[6,7] A formulation of this type has been incorporated into standard finite-element schemes for membranes,[8] however only the in-plane deformation in the wrinkled regions can be predicted with this approach. A generalisation of this theory in the context of a saturated elasticity theory has been recently proposed.[9]

In the above solutions the membrane is always modelled as a *no-compression material with negligible bending stiffness*, which amounts to assuming that a wrinkled membrane will form an infinite number of infinitesimally small wrinkles. Inspired by an analytical solution of the gravity-induced wrinkling in a hanging blanket,[10] which for the first time had considered a critical compressive stress in the membrane, we have recently proposed a simple theory[11] to predict wrinkle wavelengths and amplitudes for a rectangular membrane in uniform shear.

This theory assumes that a membrane with Young's Modulus E, Poisson's ratio ν, and thickness t carries a uniform, compressive principal stress, σ_2, equal to the buckling stress of an infinitely wide, thin plate of length λ

$$\sigma_2 = -\frac{\pi^2 E t^2}{12(1-\nu^2)\lambda^2} \tag{1}$$

Based on this assumption, it can then be shown that the wrinkle half-wavelength, λ, of a membrane subject to a shear displacement δ, as shown in Figure 1, and hence to a *shear angle*, γ, defined by

$$\gamma = \delta / H \tag{2}$$

is accurately predicted by

$$\lambda = \sqrt{\frac{\pi H t}{\sqrt{3(1-\nu^2)\gamma}}} \tag{3}$$

The wrinkle amplitude, A, is given by

$$A = \sqrt{\frac{2(1-\nu)Ht\sqrt{\gamma}}{\pi\sqrt{3(1-\nu^2)}}} \tag{4}$$

Hence, λ is inversely proportional and A directly proportional to the fourth root of the shear angle, and both of them are directly proportional to the square roots of the length and thickness of the membrane. Note that both quantities are independent of the Young's Modulus of the membrane.

Numerical Approach

Closed-form solutions based on the theoretical approaches described in the previous section exist only for simple boundary conditions. For more complex

geometries, numerical solutions are the only viable option. The first finite element algorithm to incorporate wrinkling theory[12,13] iteratively modified the membrane stiffness until all compressive stresses had been eliminated. Three different states of the membrane, namely taut, wrinkled, and slack were considered. A recent extension of this approach[14] has implemented a user subroutine that exploits the powerful numerical solvers currently available in commercial FE packages, e.g. ABAQUS and NASTRAN, and obtained successful predictions of the shape and pattern of the wrinkle regions in a square membrane subjected to point loads and inflated balloons of different shapes.

A different scheme that models the membrane as a no compression material in a non-linear geometrical analysis has been successful in simulating the shapes of inflated air-bags,[15] including the formation of some large "folds" in the surface and also of extensive wrinkled regions.

A penalty tension field parameter has been used to approximate the stress state in a parachute during deployment; modelling issues, including the influence of the order of integration and local remeshing in the wrinkled regions, have been discussed.[16] A discrete bar network model of simple membrane structures has been proposed.[17]

After testing many different wrinkling criteria, several authors have concluded that a combined stress-strain criterion is the best way of modelling real wrinkled membrane.

A general feature of all of these numerical studies is that they adopt a purely two-dimensional model of the membrane. This approach can accurately predict the stress distribution in the membrane, including wrinkled regions, and also the extent of these regions, but it can provide no information on wrinkle details. We believe that the only way of addressing this shortcoming in full is by modelling the membrane with shell elements instead of membrane elements. Of course, this considerably increases the complexity of carrying out a successful simulation.

Experimental Approach

Early experiments on wrinkled membranes focussed on the measurement of overall response parameters, such as the end rotation of a pressurized cylinder in pure bending[5] or the torque-rotation relationship of a stretched circular membrane attached to a central hub.[5,18]

Performing detailed measurements on thin membranes is not easy, mainly because high accuracy non-contact measurement apparatus is needed. A set of carefully planned experiments, including accurate measurements of wrinkle details, were carried out very recently on a square membrane subjected to different combinations of shear and tension forces.[19] These experiments showed that both the wrinkle amplitude and the number of wrinkles increase with the applied shear force, but decrease with the tension force. The reverse relationship was found between the wrinkle wavelength and the applied forces. Selected results from these experiments will be used to validate our solution method, in the section Validation of Finite Element Results: Comparison with an Experiment.

The measurement technique introduced by Jenkins et al.[19] has been extended to square membranes subjected to four corner point loads, to include the effect of thermal gradients within the membrane.[20]

Finite Element Modelling Technique

The bending stiffness of a membrane, although very small, plays a key role in determining the shape and amplitude of the wrinkles. It is essential to include this stiffness in any model that aims to capture this kind of detail, hence the obvious choice is to model the membrane with shell elements.

All analyses presented in this paper were carried out with the ABAQUS[21] commercial package. This package offers several different shell elements, and preliminary runs were carried out with 3-node triangular and 4-node quadrilateral full integration general purpose elements (S3, S4); these elements have six degrees of freedom at each node. 4-node and 9-node reduced integration thin shell elements (S4R5, S9R5), with five degrees of freedom per node, were also investigated.

The S3 element uses constant bending and membrane strain approximations, therefore a very fine mesh is required to capture the bending deformation due to wrinkling. Note that the fineness of the discretisation that is required is related to the expected wrinkling wavelength. The formulation of element S4 is similar to S3 for bending, but the in-plane strain field has been enhanced to eliminate shear locking effects. This, however, has the effect of making the element too stiff in-plane. Both S4R5 and S9R5 are thin shell elements with three in-plane translations and two in-plane rotation components, and use reduced integration with hourglass control to avoid shear locking. Both elements can model thin shells fairly accurately and S4R5 was chosen since it is computationally more economical. Also, in general it is best to avoid higher-order elements in highly geometrically non-linear problems.

A wrinkling analysis is typically performed in three stages, as follows, after —of course— defining the finite element mesh, type of elements, and material properties.

Initial Conditions

The initial stage consists in applying a small uniform prestress to the membrane, to stabilize it. The shell elements are very thin and hence their bending stiffness is so small that obtaining meaningful results when in-plane loads are applied can be a real challenge.

It is important that the amount of prestress applied at this stage should be large enough to successfully steer the subsequent buckling mode analysis, but without significantly affecting the final results.

After applying the initial prestress, a static, geometrically non-linear equilibrium check (*STATIC, NLGEOM) is carried out, to allow a small re-distribution of the state of prestress, together with small in-plane displacements.

Eigenvalue Buckling Analysis

The next step of the analysis consists in determining the buckling mode shapes of this lightly stressed membrane. These modes are then used to seed small imperfections that will trigger the formation of wrinkles in the subsequent geometrically non-linear analysis.

An eigenvalue buckling analysis (*BUCKLE) is used to predict the possible wrinkling modes of the membrane subjected to its actual boundary conditions and loading. The loading is typically defined in terms of a set of applied forces or displacements at the edge of the membrane, and has to represent the loads on the real structure. It is important that both the initial stresses and displacements from the previous stage of the analysis, as well as those due to the applied load, should be included in the calculation of the tangent stiffness matrix; this is done by default in ABAQUS. The eigenvalues and eigenvectors of the tangent stiffness matrix correspond to the load magnitudes and shapes of the possible wrinkling modes of the membrane.

After computing the possible wrinkling modes, a linear combination of some selected eigenmodes is introduced as a geometrical imperfection into the structure. The eigenvectors corresponding to the lowest eigenvalues are often those of greatest interest, and so normally the imperfections that are seeded in a structure are obtained as linear combinations of these particular eigenvectors. However, the lowest eigenvalue corresponds to the first buckling load, i.e. the load which causes the first wrinkle to form; this is not the objective of our study. The first wrinkle forms almost as soon as the load is applied, but we are interested in following the evolution of this first wrinkle, leading to the formation of a second one, and so on until a large number of wrinkles is obtained. Therefore, we base our choice of the imperfection modes that are introduced in the membrane on the expected, final wrinkling pattern and so we choose those eigenmodes which more closely resemble the diagonal wrinkle pattern that we aim to predict.

Once the appropriate eigenmodes shapes have been chosen, geometrical imperfections in the form of out-of-plane deformations are introduced (*IMPERFECTION):

$$\Delta z = \Sigma_i w_i \phi_i \tag{5}$$

where w_i is the i^{th} eigenmode and ϕ_i is a scaling factor whose magnitude is chosen as a proportion of the thickness of the membrane. Values between 1% and 100% of the thickness have been used, considering different imperfection magnitudes to test the sensitivity of the predicted response.

Post-wrinkling Analysis

A geometrically non-linear (*NLGEOM) incremental analysis is carried out under edge displacement incrementation, using the Newton-Raphson solution method. Since the equilibrium path of the wrinkled membrane includes many unstable branches, each corresponding to a localised snap-through due to the formation of an additional wrinkle, the only type of solution algorithm able —in theory— to compute the response of the structure in full is the Riks method. The response of the structure cannot be computed in full if the displacement is increased monotonically. However, all attempts to use the arc-length solution method in ABAQUS (*RIKS) were unsuccessful — possibly because wrinkling is a highly localized type of instability— and hence monotonic displacement incrementation was the only remaining option.

Automatic stabilization was provided through the STABILIZE function available in ABAQUS. This option automatically introduces pseudo-inertia and pseudo-viscous forces at all nodes when an instability is detected. Then, instead of continuing with the quasi-static analysis, ABAQUS automatically switches to a dynamic integration of the equations of motion for the structure, thus reducing the likelihood of numerical singularities.

The fictitious viscous forces that are introduced by the stabilize function are calculated on the basis of the model's response in the first increment of the analysis step, by assuming that the energy to be dissipated is a fraction of the strain energy during the first step. This fraction is called *damping intensity* and has a default value of 2×10^{-4}. To achieve good accuracy, it is generally desirable to set this parameter to the lowest possible value for which convergence can still be achieved.

Analysis of Membrane in Shear

A rectangular membrane with the dimensions defined in the section Background, see Figure 1 and Table 1, has been analysed for a 3 mm translation of the upper edge. Figure 2 shows the finite element mesh; each element has approximately unit aspect ratio.

The initial step stabilized the membrane by applying a uniform prestress $\sigma_y = 1.7$ N/mm^2, which was achieved by moving the upper edge by 0.05 mm in the y-direction.

Next, an eigenvalue buckling analysis was carried out with a prescribed horizontal displacement of 3 mm at the upper edge. Earlier analyses had shown that the eigenmodes corresponding to eigenvalues smaller than

Table 1 Properties of Kapton foil

Length, L (mm)	380
Height, H (mm)	128
Thickness, t (μm)	25
Young's Modulus, E (N/mm^2)	3530
Poisson's ratio, ν	0.3
Density, ρ (kg/mm^3)	1.5×10^{-6}

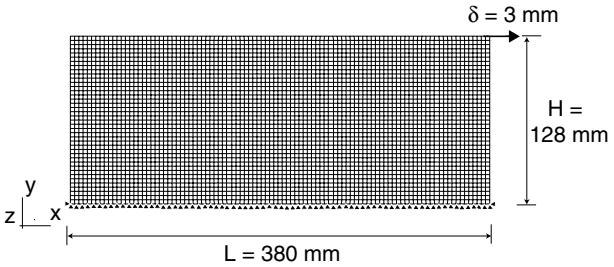

Fig. 2 Finite element mesh.

Table 2 Effect of imperfection magnitudes

$\phi_1, \ldots, \phi_4$	w_{max} (mm)	w_{min} (mm)
$0.025t$	1.12	-1.49
$0.125t$	1.09	-1.49
$0.250t$	1.14	-1.51

0.2 correspond to local deformation modes of the membrane, and hence are of no interest for the wrinkling analysis. Hence, the Lanczos solver in ABAQUS was set to produce only eigenmodes whose eigenvalues are greater than 0.2; the first four are presented in Figure 3. Note that all of these modes closely resemble the expected wrinkled pattern.

In order to test the sensitivity of the model to the amplitude of the prescribed imperfections, many different combinations of eigenmodes and scaling factors were considered. For each set, a complete wrinkling simulation was carried out and the maximum and minimum out-of-plane displacements, w_{max} and w_{min}, were computed; some sample values are given in Table 2. Note that the out-of-plane displacements are practically unchanged when the magnitude of the imperfection is increased by a factor of 10. Also note that the particular displacements listed in the table correspond to the largest two wrinkles, on either side of the membrane, but the smaller wrinkles between these large ones were also found to have the same amplitude and wavelength, regardless of the size of imperfection.

It was thus concluded that the particular magnitude of the imperfection that is chosen is not critical and it was decided to use a "standard" imperfection consisting of the first four eigenmodes corresponding to eigenvalues greater than 0.2, normalised by ABAQUS, each multiplied by a scaling factor $\phi_i = 0.125t$.

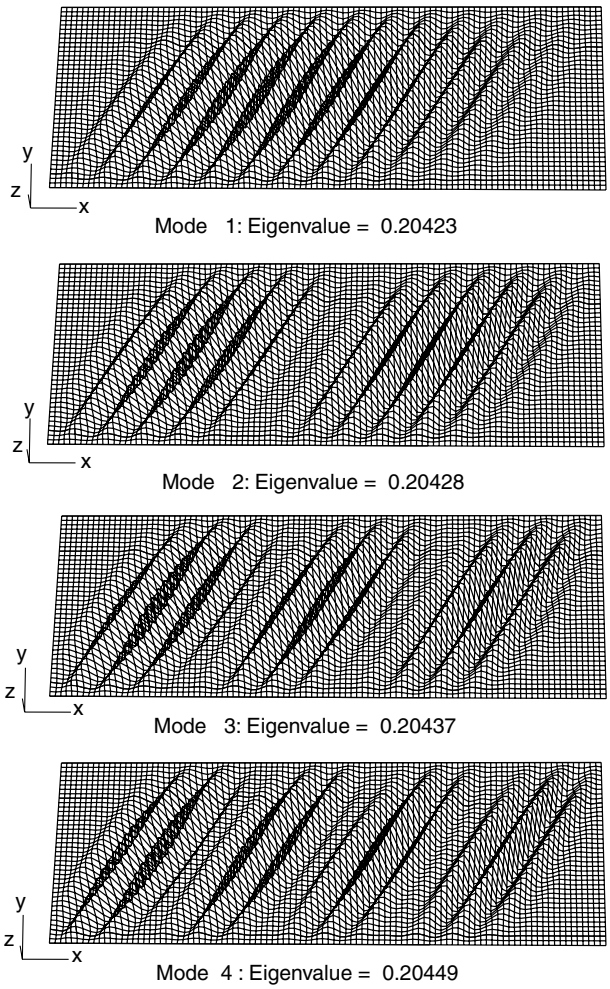

Fig. 3 First four eigenmodes with eigenvalue > 0.2**.**

The parameter that controls the amount of numerical damping introduced by ABAQUS in case of an instability has the default value 2×10^{-4}. It was reduced to 1×10^{-8} using *STABILIZE, FACTOR $= 1 \times 10^{-8}$ to minimize the deviation between the computed equilibrium path and the actual path.

Finally, three different mesh sizes were used to investigate the effect of mesh density on the final wrinkled shape. It was observed that there is no change in the number of wrinkles when, starting from a reference mesh with 6950 elements, the number of elements is roughly doubled. However, if the number of elements is halved a smaller number of wrinkles is predicted, see Table 3, which suggests that the reference mesh is sufficiently fine to produce mesh-independent results. Since the computational time increases roughly proportionally to the number of elements, it would be pointless to use a mesh finer than the reference one.

Overall Behaviour

Figure 4 shows a plot of the total shear force applied to the membrane versus the shear displacement imposed. Note that the global behaviour of the mem-

Table 3 Number of wrinkles for different meshes

No. elements	Total dof's	No. wrinkles
3960	19800	15
6950	34750	17
13134	65670	17

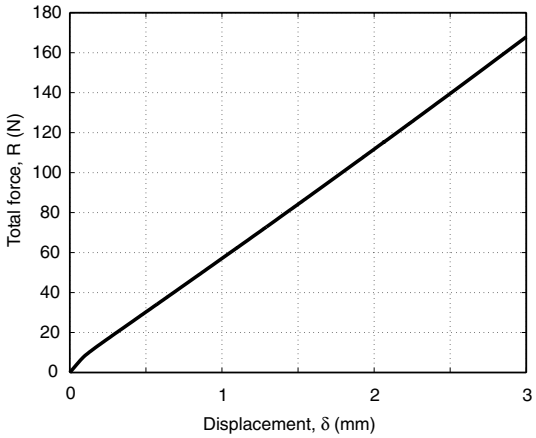

Fig. 4 Overall force-displacement relationship.

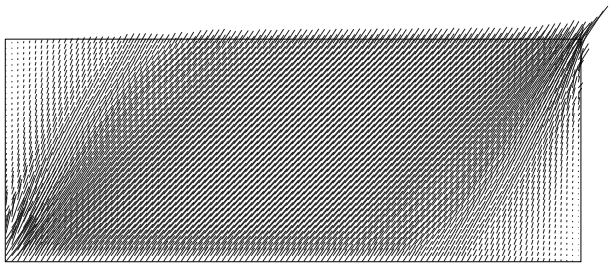

Fig. 5 Principal stress directions and magnitudes.

brane is essentially linear, although a slight softening can be observed near the origin. This corresponds to the formation of the first set of wrinkles, and signals the end of the purely in-plane behaviour of the membrane. The initial in-plane shear stiffness is 101 N/mm, which decreases by about a third.

A vector plot of the stress distribution corresponding to the final displacement of 3 mm is shown in Figure 5. For each element, the directions and magnitude of the two principal stresses have been plotted, but in fact the major stress, σ_1, is so much larger than the minor stress, σ_2, that only one vector shows. The direction of the major principal stress corresponds to the direction of the wrinkles, which are clearly inclined at 45° and uniform in the central part of the membrane. Near the side edges there are two lightly stressed triangular regions, but the top-right and bottom-left corners act as stress risers, with stress concentrations of up to 2.5.

A deeper understanding of the stress distribution in the wrinkled membrane can be obtained by considering the principal stresses across the mid-height section

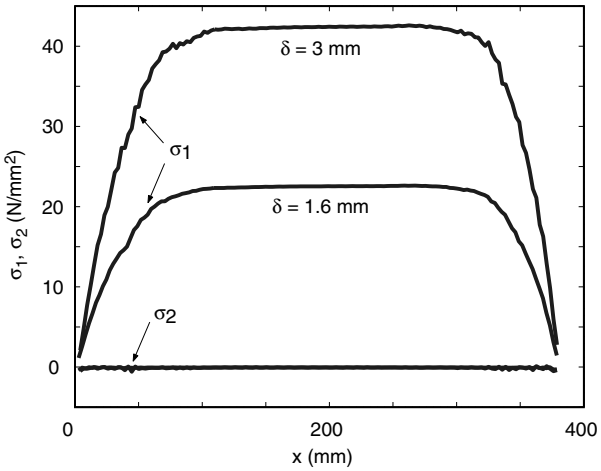

Fig. 6 Principal mid-plane stresses across mid-height section.

($y = 64$ mm). Figure 6 shows plots of the major and minor principal stresses through the mid-plane of the membrane for two different values of the shear displacement. The plots show that σ_1 increases rapidly —starting from zero at the edges— to an approximately uniform, positive value, whereas σ_2 remains very small.

In fact the mid-plane, minor principal stress is negative and roughly uniform in each case. It can be predicted with Equation 1, as discussed in the section Background: Analytical Approach.

Detailed Behaviour

The post-wrinkling behaviour of a rectangular membrane in shear shows some very interesting effects, which become apparent if one looks closely enough.

When the shear displacement is gradually increased the wrinkles grow in amplitude, then become unstable, and then generate even more wrinkles with smaller wavelength. A complete history is shown in Figure 7; this is a plot of δ vs. the position of the points of maximum and minimum out-of-plane displacement, i.e. the crests and troughs of the wrinkles, across the mid-height section of the membrane.

Note that the solid lines on the two sides of the plot are almost straight and vertical, indicating that the edge wrinkles do not move. Looking further in, towards the centre of the plot, the first dotted line and the second solid line are continuous, but gently curved outwards. All other lines contain one or more bifurcation points, which indicates that additional wrinkles are created. The first five bifurcations occur very quickly, at the start of the simulation; afterwards the values of δ associated with each jump can be clearly identified, and are labelled (6)–(10). As the number of wrinkles increases the membrane becomes more stable and hence a greater increase of δ is required to get to the next bifurcation.

Because the wrinkles can most easily reorganise

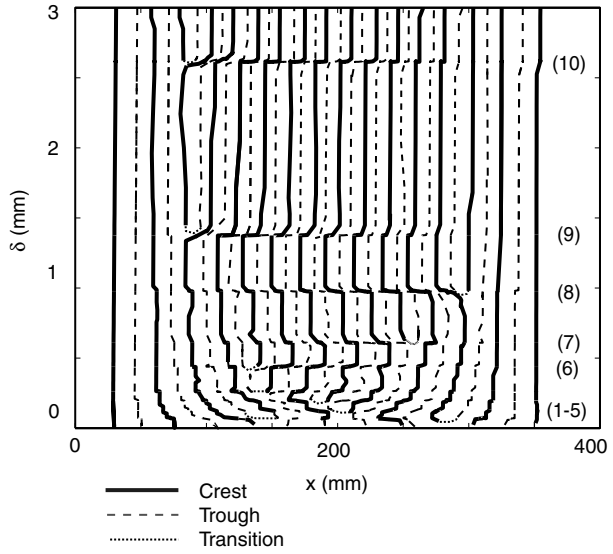

Fig. 7 Trajectories of w_{max} and w_{min}.

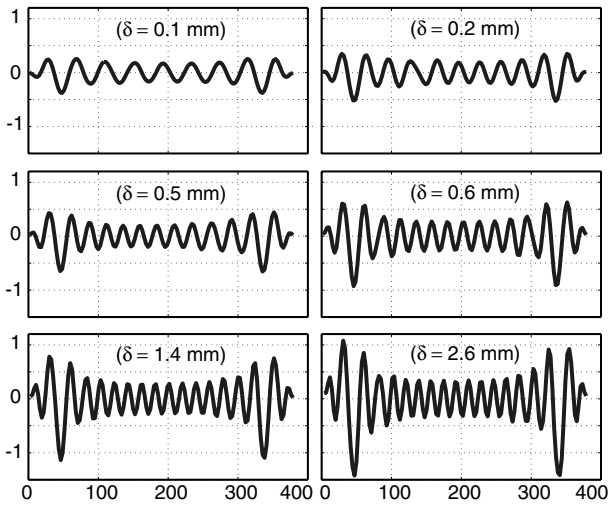

Fig. 8 Mid-height cross-sections for different δ's.

themselves in the middle of the membrane, new wrinkles tend to appear in this region. The large wrinkles on the sides do not move, as they are "pinned" by the corner supports.

Figure 8 shows different shapes of the mid-height section of the membrane, as δ is increased. The particular shapes shown here were obtained immediately after the bifurcations labelled (2), (4), (6), (7), (9) and (10) in Figure 7. The *number of wrinkles*, defined as the number of crests in each plot, is 9, 11, 13, 14, 16 and 17 respectively. Note that the wrinkle amplitude in the central region increases from 0.13 mm to 0.33 mm in these plots, while the wavelength obviously decreases.

The transition from one shape to the next is not smooth, but is triggered by a local instability that leads to mode jumping; this behaviour can also be observed in an experiment. The sequence of jumps is seen

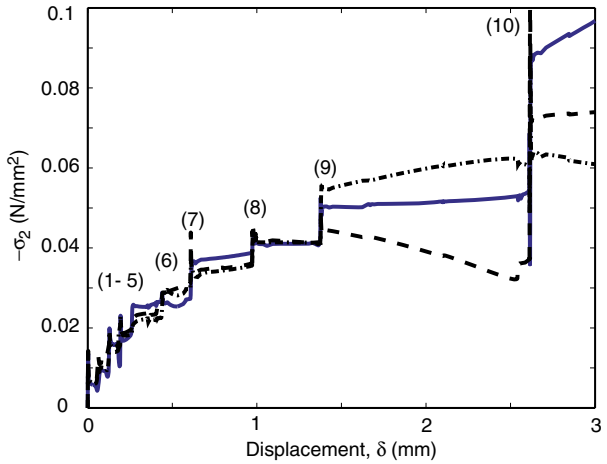

Fig. 9 Plot of minor principal stresses, showing evidence of mode jumping.

most clearly in a plot of the *minor* principal stress, σ_2, at a representative point of the membrane vs. the shear displacement, as shown in Figure 9. Here the stresses at three points near the centre of the membrane have been plotted. Which particular point is chosen is not significant, but jumps that are associated with an instability that is far away from the chosen point may not show; therefore, it is useful to monitor the stress at several points. Note that σ_2 is always compressive; also note that it would have been pointless to plot the major principal stress, which is too large for the jumps to show.

Figure 9 clearly shows ten jumps, numbered (1)–(10). Jump (1) occurred almost immediately after displacing the upper edge. This indicates that the bending stiffness of the membrane is so small that wrinkles start forming immediately. Due to the geometric imperfections introduced in the membrane, the first jump is directly to a configuration with seven wrinkles. This is followed in rapid sequence by jumps (2)–(5); then the membrane settles in a more stable state. It is interesting to note that, as the membrane becomes more stable, σ_2 remains almost constant between consecutive jumps.

From a numerical simulation viewpoint, it should be noted that jumps (1)–(6) occur at almost equal stress levels, hence it is likely that secondary bifurcation paths exist in this region. In some cases it was found that the solution diverges, then the analysis had to be restarted after increasing the damping intensity factor to 1×10^{-7}. This allowed the analysis to continue, but then the damping intensity had to be decreased before the next jump. Varying the numerical damping in a simulation has the effect of creating a certain amount of hysteresis, whose effects can be seen by cyclically loading and unloading the membrane.

Now, let's look more carefully into the mode-jumping. Figure 10 shows an enlarged view of the

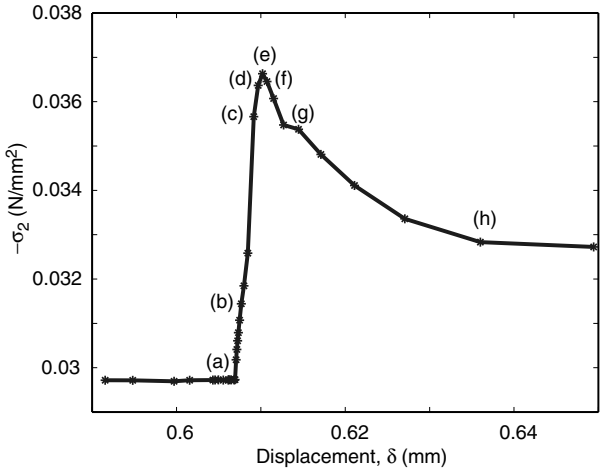

Fig. 10 Compressive stress during jump (6).

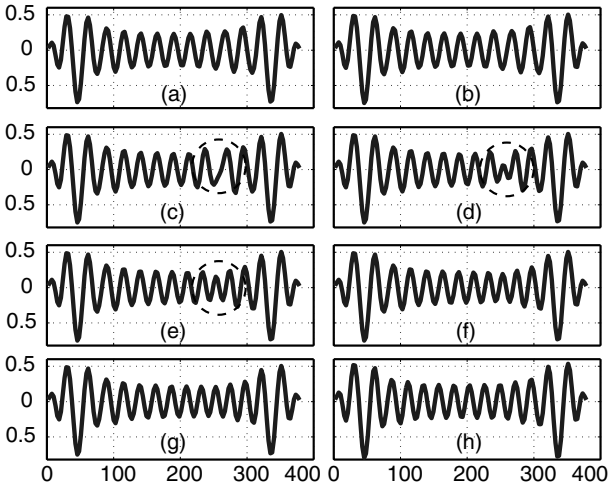

Fig. 11 Variation of mid-height cross section during jump (6).

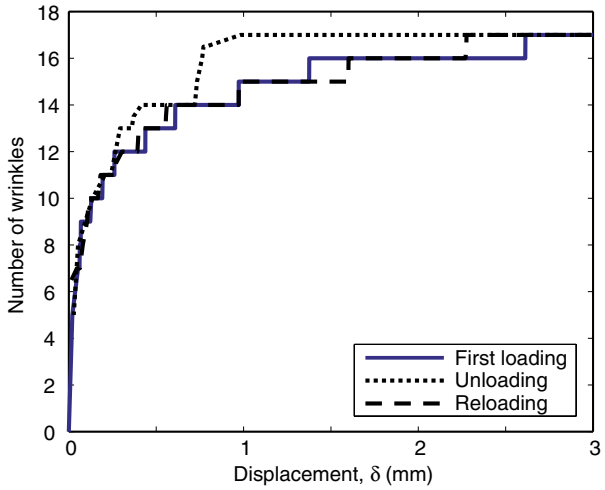

Fig. 12 Number of wrinkles during load cycling.

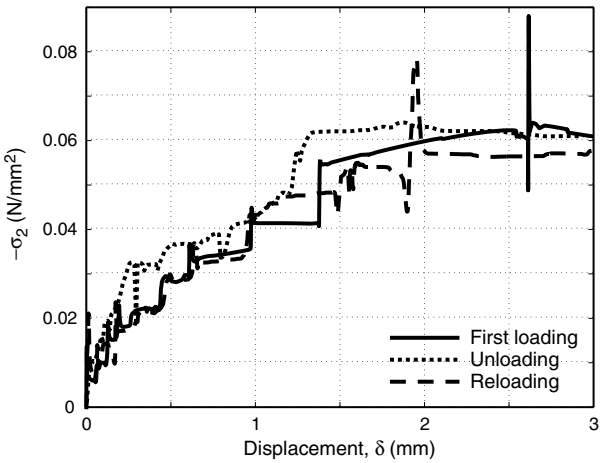

Fig. 13 Compressive stress during load cycling.

stress-displacement plot near jump (6); eight points —labelled (a)–(h)— have been marked on the equilibrium path and the corresponding mid-height cross-sections are shown in Figure 11.

This sequence of cross sections shows that the 13 wrinkles that had formed previously remain stable until σ_2 has almost reached a peak, at point (c). Here a small asymmetry begins to appear in the cross-sectional plot, which rapidly grows into a new wrinkle (d)–(e). Thus, the transition from 13 to 14 wrinkles occurs over a very small displacement increment and then the new mode stabilizes itself while the magnitude of σ_2 rapidly decreases.

It is also interesting to investigate the behaviour of the membrane during a simulated loading–unloading cycle. Figure 12 shows the variation in the number of wrinkles when the shear displacement is increased from 0 to 3 mm, and then decreased to 0, and finally increased again to 3 mm. Figure 13 shows the corresponding plot of the stress σ_2 at an element in the middle of the membrane. Note that during unloading the wrinkles tend to *stay on*, thus the final number of wrinkles does not start decreasing until the shear displacement has been reduced to $\delta = 0.8$ mm, at which point the number of wrinkles suddenly decreases from 17 to 14. Thus, the behaviour on unloading is different from loading. The stress variation is also much smoother during unloading, see Figures 12–13.

During reloading the membrane generally follows the same path as during first loading, however, the final configuration with 17 wrinkles is achieved slightly earlier this time. This may be due to the effect of the geometrical imperfections left in the membrane at the end of the first load cycle, which may have facilitated the formation of the "correct" pattern of wrinkles. Also note that the stabilisation factor varies during each simulation, and also during load reversal; it is difficult to quantify the effect of this variation.

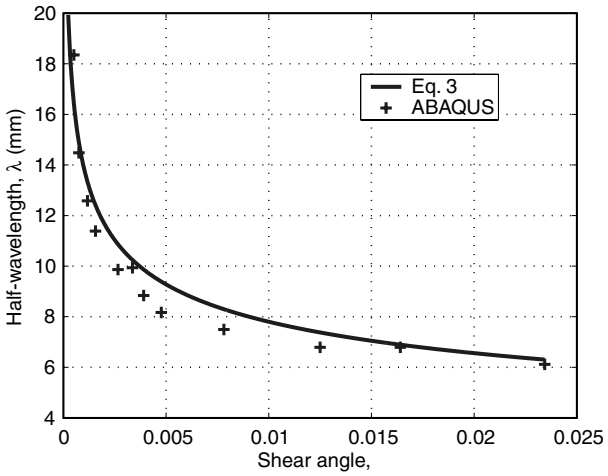

Fig. 14 Comparison of wrinkle wavelengths.

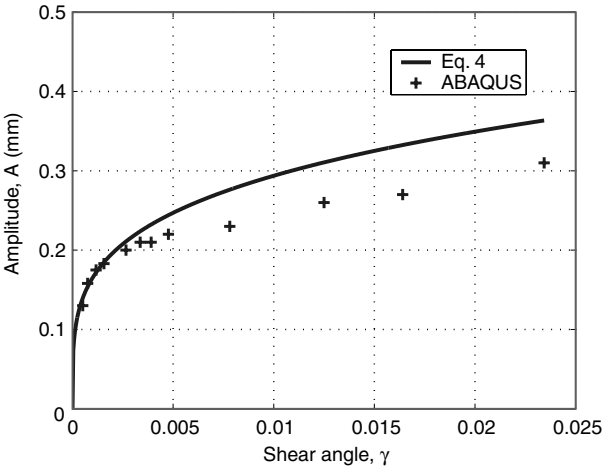

Fig. 15 Comparison of wrinkle amplitudes.

Validation of Finite Element Results

The results obtained from the ABAQUS simulation will be compared to the predictions from (i) the approximate analytical model of Wong and Pellegrino[11] and (ii) a recently published experiment.[19]

Comparison with Analytical Solution

Figures 14 to 16 compare the variation of the wrinkle half-wavelength and amplitude, and of the minor principal stress with the shear angle in a rectangular membrane with the properties listed in Table 1. Each figure shows both an analytically predicted curve, from Equation 1, 3, and 4, respectively, plus 13 results from an ABAQUS simulation.

The wrinkle wavelength and amplitude were extracted from the ABAQUS output by plotting the mid-height cross section, selecting visually the uniformly wrinkled region, and finally measuring the average wavelength and amplitude off each plot. The stress values were obtained by averaging over the the central half of the cross section.

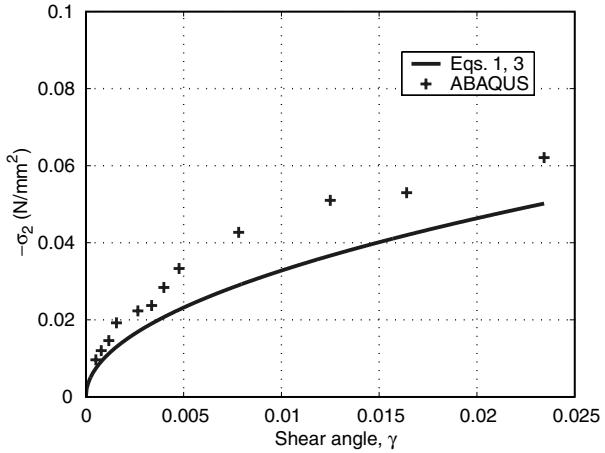

Fig. 16 Comparison of mid-plane compressive stresses.

It can been seen that the half-wavelengths λ obtained from ABAQUS agree extremely closely with the analytical predictions made over the whole range of γ. The wrinkle amplitudes are very close for $\gamma < 0.005$, but then diverge by up to 0.05 mm although they follow similar trends.

The variation of the minor principal stress predicted by ABAQUS also follows the same trend as the analytical model. The two predictions are very close for $\gamma < 0.004$. For larger shear angles discrepancies of up to 30% are observed, particularly for intermediate values of γ.

Comparison with an Experiment

The next test of the finite element modelling technique presented in this paper was based on an experimental study of a square Mylar foil with side length of 228.6 mm, subjected to a combination of tension and shear forces.[19] The experimental setup, shown in Figure 17, consisted of two straight edges (grippers), one attached to a rigid foundation, the other controlled by two stepper motors. The axial and shear forces applied to the membrane, in the x and y-directions respectively, are measured by force transducers and monitored by a computer-controlled system. A capacitance displacement sensor was used to measure the profile of the membrane at a distance of 100 mm from the stationary gripper.

A variety of experiments were conducted, with shear loads in the range 0–5 N and axial loads in the range 1–5 N.[19] The load case chosen to test our simulation consists of a shear load of 4 N and a tension load of 5 N.

An ABAQUS model of the membrane was set up, consisting of 9900 S4R5 shell elements; the grippers were assumed to be made of Aluminium and modelled with beam elements, type B21. The beam elements were connected to the edge of the shell elements using the Multi Point Constraint (*MPC, TIE) option in

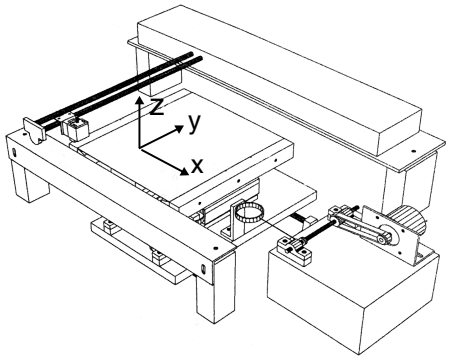

Fig. 17 Experimental set-up.[19]

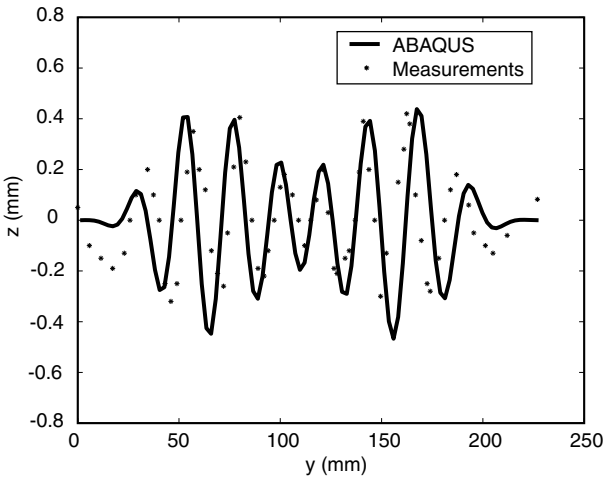

Fig. 18 Comparison between ABAQUS results and measurements by Jenkins et al.[19]

ABAQUS. The same loading conditions as in the experiment were simulated, by first stretching the membrane in the x-direction until the full axial load had been applied and by then applying the shear load as a separate step while the axial force was kept constant. During the first step, translation in the x-direction only was allowed, whereas in the second step both x and y-translations of the moving edge were allowed.

Figure 18 compares the measured out-of-plane deformation for this load case,[19] with the ABAQUS results.

It can be seen that away from the edges the ABAQUS model predicts the wrinkle wavelength and amplitudes very accurately. Near the edges there is a mismatch, mainly because the out-of-plane translation of the free edges had to be restrained in the simulation, to avoid singularities, whereas in the experiment they were left unrestrained. Also, in the experiment a small, unknown prestress had been applied to eliminate initial wrinkling; in the simulation an arbitrary prestress of 0.25 N was applied, i.e. 5% of the total tension, during the first stage.

A more detailed comparison of experiment and simulation is presented in Table 4.

Table 4 Comparison of simulation and experiment

	Jenkins	ABAQUS
No. of wrinkles	8	8
Amplitudes (mm)	0.18–0.42	0.23–0.42
Half-wavelength (mm)	7.94	10.7
Wrinkle angles*	35.5°	36°

Discussion and Conclusions

The finite element simulation technique presented in this paper has been shown to be robust and capable of producing good quality results. Regarding the validation that has been presented, a key point to note is that neither the analytical solution is exact — indeed, it is only a simple approximate solution— nor the experimental comparison can be guaranteed to be absolutely error free. Of the two, the latter is likely to be the most accurate and, disregarding the differences associated with the side edges, the results from the ABAQUS simulation in Fig. 18 agree almost perfectly.

The detailed implementation of our simulation procedure is not straightforward but, with the details provided in this paper, it is hoped that anybody sufficiently familiar with ABAQUS will be able to reproduce and extend our results.

The potential usefulness of our simulation technique goes beyond the computation of the wrinkle details. Having been able to "look inside" the membrane and plot —for example— the compressive stress across the wrinkles has provided a convincing backing for the assumption, made in our earlier study,[11] that the average principal compressive stress in a uniformly wrinkled membrane is approximately given by Equation 1. Being able to do this sort of thing makes it possible to identify features of the complex behaviour of thin membranes that need to be included in simple models, which can be very useful.

Acknowledgments

We thank Professor C.R. Calladine for many useful suggestions. Financial support for Y.W.W. from the Cambridge Commonwealth Trust is gratefully acknowledged.

References

[1]Wagner, H., "Flat sheet metal girder with very thin metal web". *Zeitschrift für Flugtechnik Motorlurftschiffahrt*, Vol. 20, 1929.

[2]Reissner, E., "On tension field theory", *Proc. V International Congress of Applied Mechanics*, pp. 88–92, 1938.

[3]Mansfield, E.H., "Tension field theory, a new approach which shows its duality with inextensional theory", *Proc. XII International Congress of Applied Mechanics*, pp. 305–320, 1968.

[4]Mansfield, E.H., *The Bending and Stretching of Plates*. Cambridge University Press, Cambridge, Second edition, 1989.

*Maximum wrinkle angles measured from side edge.

[5]Stein, M. and Hedgepeth, J.M., "Analysis of partly wrinkled membranes", *NASA TN D-813*, 1961.

[6]Pipkin, A.C., "The relaxed energy density for isotropic elastic membranes", *IMA Journal of Applied Mathematics*, Vol. 36, pp. 85–99, 1986.

[7]Steigmann, D.J., "Tension field theory", *Proceedings of the Royal Society of London, A*, Vol. 429, pp. 141–173, 1990.

[8]Barsotti, R. and Ligaro, S.S., "An accurate wrinkled membrane model for analysing the post-critical behaviour of stiffened plate-girders", In *Proc. IASS-IACM 2000 Computational Methods for Shells and Spatial Structures*, (Edited by M. Papadrakakis, A. Samartin and E. Onate), pp. 1–16.

[9]Epstein, M. and Forcinito, M.A., "Anisotropic membrane wrinkling: theory and analysis", *International Journal of Solids and Structures*, Vol. 38, pp. 5253–5272, 2001.

[10]Rimrott, F.P.J. and Cvercko, M., "Wrinkling in thin plates due to in-plane body forces", *IUTAM Symposium on Inelastic behaviour of Plates and Shells*, Rio De Janeiro, 1985.

[11]Wong, Y.W. and Pellegrino, S., "Amplitude of wrinkles in thin membrane". To be published in: *New Approaches to Structural Mechanics, Shells and Biological Structures*, (Edited by H. Drew and S. Pellegrino), Kluwer Academic Publishers, 2002.

[12]Miller, R.K. and Hedgepeth, J.M., "An algorithm for finite element analysis of partly wrinkled membranes", *AIAA Journal*, Vol. 20, pp. 1761–1763, 1982.

[13]Miller, R.K., Hedgepeth, J.M., Weingarten, V.I., Das, P. and Kahyai, S., "Finite element analysis of partly wrinkled membranes", *Computers and Structures*, Vol. 20, pp. 631–639, 1985.

[14]Adler, A.L., Mikulas, M.M., and Hedgepeth, J.M., "Static and dynamic analysis of partially wrinkled membrane structures". *Proc. 41st AIAA/ASME/ASCE/AHS/ASC Structures, Structures Dynamics, and Material Conference and Exhibit*, Atlanta, GA, 3-6 April 2000, AIAA-2000-1810.

[15]Contri, P. and Schrefler, B.A., "A geometrically non-linear finite element analysis of wrinkled membrane surfaces by a no-compression material model", *Communications in Applied Numerical Methods*, Vol. 4, pp. 5–15, 1988.

[16]Liu, X, Jenkins, C.H. and Schur, W.W., "Computational issues in the modelling of wrinkling during parachute deployment", In *IUTAM-IASS Symposium on Deployable Structures: Theory and Applications*, (Edited by S. Pellegrino and S.D. Guest), Kluwer Academic Publishers, pp. 239–250, 2000.

[17]Yang, B., Ding, H., Lou, M. and Fang, H., "A new approach to wrinkling prediction for space membrane structures", *Proc. 42nd AIAA/ASME/ASCE/AHS/ASC Structures, Structural Dynamics, and Materials Conferenceand Exhibit*, Seattle, WA, 6-19 April 2001, AIAA-2001-1348.

[18]Mikulas, M.M., "Behavior of a flat stretched membrane wrinkled by the rotation of an attached hub", *NASA TN D-2456*, 1964.

[19]Jenkins, C.H., Haugen, F. and Spicher, W.H., "Experimental measurement to wrinkling in membranes undergoing planar deformation", *Experimental Mechanics*, Vol. 38, pp. 147–152, 1998.

[20]Blandino, J.R., Johnston, J.D., Miles, J.J. and Soplop, J.S., "Thin-film membrane wrinkling due to mechanical and thermal loads", *Proc. 42nd AIAA/ASME/ASCE/AHS/ASC Structures, structural Dynamics, and Materials Conference and Exhibit*, Seattle, WA, 16-19 April 2001, AIAA-2001-1345.

[21]Hibbit, Karlsson and Sorensen, Inc., *ABAQUS Theory and Standard User's Manual*, Version 6.2, Pawtucket, RI, USA, 2001.